Machine Learning-Based Prediction of Soil Electrical Resistivity Using Field-Instrumented Hydrologic Data

Md. Jobair Bin Alam, Ph.D., P.E., M.ASCE[1]; Robi Sonkor Mozumder, S.M.ASCE[2]; Chukwuzubelu Okenwa Ufodike, Ph.D.[3]; and Naima Rahman, Ph.D., P.E.[4]

[1]Associate Professor, Dept. of Civil Engineering, Prairie View A&M Univ., TX. Email: mdalam@pvamu.edu
[2]Graduate Research Assistant, Dept. of Civil Engineering, Prairie View A&M Univ., TX. Email: rmozumder@pvamu.edu
[3]Assistant Professor, Engineering Technology and Industrial Distribution, J. Mike Walker '66 Dept. of Mechanical Engineering and Dept. of Multidisciplinary Engineering, Texas A&M Univ., College Station, TX. Email: ufodike@tamu.edu
[4]Project Professional, SCS Engineers, Houston, TX. Email: nrahman@scsengineers.com

Downloaded from ascelibrary.org by Md Jobair Bin Alam on 03/10/26. Copyright ASCE. For personal use only; all rights reserved.

ABSTRACT

Subsurface characterization is challenging due to soil heterogeneity and the complex interplay of moisture, suction, and temperature. The ability to deduce these variables through a single measurable soil property, specifically soil resistivity, can potentially enhance subsurface characterization. This study aimed to investigate the relationship between field-surveyed soil electrical resistivity and basic soil physical properties to develop a predictive model using various machine learning-based regression techniques. To achieve this objective, moisture and temperature sensors, along with tensiometers, were installed at different depths in several vegetated soils, and resistivity tests were conducted periodically at the same locations. Two regularized linear regression models, Ridge (L2 penalty) and Lasso (L1 penalty), were then developed and compared to predict bulk resistivity from the three hydrological variables. All predictors were standardized before analysis, and hyperparameters were optimized via five-fold cross-validation. The performance of the two regression techniques was evaluated using the metrics Root Mean Square Error (RMSE) and Coefficient of Determination (R^2). Results obtained from the study indicated that Ridge regression achieved the highest predictive accuracy (R^2 = 0.778; RMSE = 14.28 Ω-m). Conversely, Lasso regression yielded a sparser model (R^2 = 0.692; RMSE = 19.40 Ω-m). The results also showed that soil suction has negligible contributions in correlating soil resistivity with soil physical properties, especially in Ridge regression. These results demonstrate that, among the tested methods, Ridge regression most reliably captures the linear relationships between hydrological state variables and soil resistivity in vegetated soil.

INTRODUCTION

Advancements in Electrical Resistivity Imaging (ERI) have significantly enhanced the understanding of moisture variations in soil suction, providing a non-invasive, high-resolution method for monitoring subsurface conditions. ERI's ability to map soil moisture and suction over large areas provides a comprehensive view of soil dynamics, which is crucial for applications such as earth infrastructures, precision agriculture, and geoenvironmental applications. This method enables high spatial resolution monitoring of subsurface conditions, making it

Downloaded from ascelibrary.org by Md Jobair Bin Alam on 03/10/26. Copyright ASCE. For personal use only; all rights reserved.

particularly beneficial for large-scale applications. It allows for the mapping of moisture content and suction parameters across extensive areas where traditional point-based sensors are impractical (Chambers et al. 2014; Alam et al. 2019). ERI has been shown to correlate well with soil suction, offering a means to estimate suction changes over large volumes. This is achieved by deriving analytical relationships between soil matric suction and electrical resistivity, which can be applied to different soil types and conditions (Piegari & Maio, 2013; Zha et al. 2010). The ability to predict matric suction from resistivity measurements provides a practical and cost-effective alternative to traditional suction measurement methods, which are often expensive and limited to small areas (Zha et al. 2010). Furthermore, soil resistivity correlates significantly with moisture content and soil suction, making it a crucial parameter in geotechnical, agricultural, and construction applications. By integrating these variables, models can better account for the dynamic nature of soil conditions, leading to more reliable predictions.

Bulk electrical resistivity of soils exhibits a strong, typically inverse, dependence on water content consistent with Archie's law (Archie, 1942). Empirically, a study (Jusoh and Osman, 2017) reported a resistivity-moisture correlation with a high coefficient of determination (R^2 = 0.8168). Controlled laboratory studies likewise show monotonic decreases in resistivity with increasing moisture due to enhanced ionic conduction within the connected pore network (Jusoh & Osman, 2017; Reddy & Chandrasekaran, 2022; Bernardi et al. 2019). Field-scale ERT measurements corroborate this relationship (Sari et al. 2014). Nevertheless, measured resistivity is also modulated by soil textural/mineralogical composition, measurement frequency, pore-fluid properties, temperature, and other environmental conditions, which should be controlled or incorporated into calibration procedures (Coelho et al. 2013; Liangfu & Binquan, 2012).

Although not explicitly detailed in the provided contexts, soil suction is known to influence soil resistivity, and including it in regression models, along with soil moisture and temperature, can improve prediction accuracy. Incorporating temperature and suction data into regression models can significantly boost the accuracy of predicting soil resistivity. Temperature has a strong influence on the EC of the subsurface (Sen and Goode, 1992). Temperature impacts soil resistivity by changing moisture content and ionic mobility. Rein et al. (2004) investigated coupled temperature–moisture effects and showed that even diurnal temperature swings can have a substantial impact. Additionally, soil suction, covering both matric and wet suction, is a measure of the soil's water retention ability and is inversely related to moisture content. Higher soil suction typically indicates lower moisture content, resulting in increased resistivity (Piegari & Maio, 2013). Empirical models, such as those proposed by van Genuchten (1980) and Archie (1942), aid in predicting these variations (Piegari & Maio, 2013). Including soil suction data in models enables a more accurate estimation of soil moisture content, a key factor in determining resistivity. This approach has been shown to improve the accuracy of soil resistivity predictions (Nnamdi & Chandima, 2023).

This research focused on exploring the relationship between soil electrical resistivity and key soil physical properties such as soil moisture, suction, and temperature based on field-scale measurements, aiming to develop a predictive model through machine learning regression techniques. Lasso and Ridge regression are two prominent techniques used to address multicollinearity in regression analysis. Both methods apply regularization to stabilize coefficient estimates, but they differ in their approach and impact on model interpretation and performance. Ridge regression adds a penalty equivalent to the square of the magnitude of the coefficients, while Lasso adds a penalty equivalent to the absolute value of the magnitude of the

Downloaded from ascelibrary.org by Md Jobair Bin Alam on 03/10/26. Copyright ASCE. For personal use only; all rights reserved.

coefficients. These differences lead to distinct outcomes in handling multicollinearity, particularly in terms of coefficient shrinkage and variable selection.

Ridge regression applies an L2 penalty, which shrinks the coefficients of correlated predictors towards each other, effectively reducing their variance without setting any coefficients to zero. This makes Ridge regression particularly useful when all predictors are believed to be relevant (Rahmawati, 2022; Schreiber-Gregory, 2018). On the other hand, Lasso regression uses an L1 penalty, which can shrink some coefficients to zero, effectively performing variable selection. This feature makes Lasso particularly useful for creating simpler, more interpretable models by excluding irrelevant predictors (Rahmawati, 2022; Dabal & Abdullah, 2021). Furthermore, Ridge regression is often preferred when multicollinearity is present, as it tends to provide more stable estimates and lower mean squared errors (MSE) compared to Lasso, especially when the sample size is large (Rahmawati, 2022; Efeizomor, 2023). However, Lasso is more effective in scenarios with severe multicollinearity, especially with smaller sample sizes, as it can eliminate redundant variables, thus simplifying the model (Altelbany, 2021; Herawati et al. 2018).

MATERIALS AND METHODS

Site Description, Instrumentation, and Field Testing

The study was conducted on six large-scale vegetated test sections measuring 12 m by 12 m and 1.2 m deep. The subgrade of an intermediate landfill cover was excavated, a geocomposite drainage layer was placed above a geomembrane layer at the subgrade bottom, and the soil was placed and compacted during the building of the test sections. Each test section was equipped with tensiometers and moisture sensors to track the field SWCC. Figure 1 displays the test section's instrumentation. The top sensor was situated 305 mm from the surface, while the moisture sensors were spaced 228 mm apart. Figure 1 illustrates how far apart the tensiometers were from one another: 457 mm. All the sensors were connected through a data logger system for continuous monitoring of soil suction from the installed sensors. The soil used on the test sections had a fine fraction (clay and silt) in the range between 82% to 96%, while the plasticity index (PI) and liquid limit (LL) ranged from 26 to 33 and 51 to 60, respectively. According to the Unified Soil Classification System (USCS), laboratory test findings classified the soil as high plastic clay (CH).

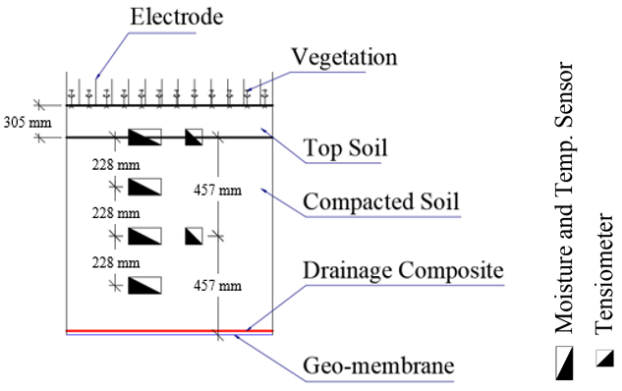

Figure 1. Schematic of instrumentation

Downloaded from ascelibrary.org by Md Jobair Bin Alam on 03/10/26. Copyright ASCE. For personal use only; all rights reserved.

Throughout the investigation period, the electrical resistivity tomography (ERT) approach was used to probabilistically characterize matric suction. The Advanced Geosciences Institute (AGI) produced programmable eight-channel resistivity equipment that was employed in this investigation. 28 electrodes in total, spaced 152 mm apart, were employed in a transect spanning 4116 mm across the sensor positions (Figure 2). To ensure that the resistivity profile is created within the 1.2 m cover and does not overlap with the geomembrane layer resting on the subgrade (bottom of cover), a narrow electrode spacing was used. Raw resistivity data were retrieved along the sensors' location. Every time the resistivity readings were recorded from the apparatus, temperature adjustments were made. Apparent-resistivity data collected with a 2D dipole–dipole array were inverted in EarthImager 2D using the software to recover true-resistivity models; all interpretations are based on the inverted sections (not raw pseudosections). For consistent visualization across profiles, the scale was fixed at 0–100 Ω·m

Figure 2. Field setup with a resistivity meter and testing

Throughout the monitoring period (two years), a monthly field ERT test was conducted. However, during the summers, the ERT test was conducted weekly since the summers had notably high temperatures and precipitation with variable frequencies and intensities. The ERT profiles at the same transect are shown in Figure 3. Only two contrasting ERT profiles are presented here: one on June 23, when high temperatures were maintained for an extended period without rain, and another on July 19, which was carried out the day following significant rainfall. There is a noticeable difference in resistivity profiles between the two in the same transect. As indicated by the red contour in Figure 3(a), the top 304.8 mm to 457.2 mm of the subsurface displays a high resistivity zone. Because the resistivity values at the bottom of the profiles are lower than those in the top 304.8 mm to 457.3 mm (approximately), this suggests the presence of moisture and consequently reduced suction. The resistivity contour in Figure 3(b) changed from a concentrated red contour to virtually green to blue, indicating a considerable fall in resistivity value and moisture incursion into the soil following precipitation events.

Data Preparation and Regularization Methods

The dataset comprised simultaneous measurements of soil resistivity (y), volumetric moisture content (x_1), matric suction (x_2), and temperature (x_3) at each sampling instant. Before model fitting, all predictor variables were standardized to a zero mean and unit variance using the following equation:

$$x_j' = \frac{x_j - \bar{x}}{SD_j}, (j = 1, 2, 3) \quad (1)$$

where $\bar{x}$ and SD_j are the sample mean and standard deviation of predictor j. Standardization ensures that the regularization penalty treats each coefficient on an equal scale. The Ridge and Lasso models solve the following regularized regression objective functions, respectively.

$$\min_{\beta_o, \beta} \sum_{i=1}^{n} \left(y_i - \beta_o - {x'_i}^T \times \beta\right)^2 + \alpha \sum_{j=1}^{3} {\beta_j}^2 \quad (2)$$

$$\min_{\beta_o, \beta} \sum_{i=1}^{n} \left(y_i - \beta_o - {x'_i}^T \times \beta\right)^2 + \alpha \sum_{j=1}^{3} |\beta_j| \quad (3)$$

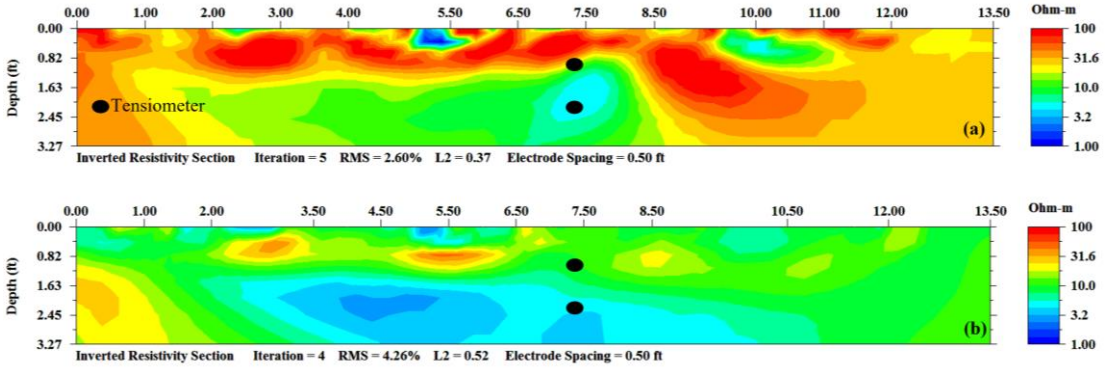

Figure 3. Resistivity imaging result for (a) 23rd June 2016, (b) 19th July 2016

Where y_i is the measured resistivity at observation i., β_o is the intercept term (i.e., the predicted resistivity when all predictors are zero), after standardization, this centers the predictions. The $x_i=(x_{i1}\ldots,x_{ip})^T$ is the p-vector of predictor values (standardized moisture, suction, temperature) for observation i. $\beta=(\beta_1\ldots,\beta_p)^T$ is the vector of regression coefficients for each predictor. The first term of the objective functions is the Residual Sum of Squares (RSS). The RSS measures the squared differences between observed and predicted resistivity; a smaller RSS indicates a better fit. The α parameter is the regularization parameter (≥0) controlling the strength of shrinkage. The L2 penalty (term 2 of the Ridge objective function): $\alpha\sum\beta_j^2$ adds a cost proportional to the square of each coefficient, shrinking all β_j toward zero to reduce variance and mitigate multicollinearity in Ridge regression. In Lasso regression, the L1 penalty (term 2): $\alpha\sum|\beta_j|$ adds a cost proportional to the absolute value of each coefficient. This encourages exact zeros in some β_j, performing variable selection and yielding a sparser model. For each model, the regularization strength α was chosen by five-fold cross-validation. Grid search over α values on a logarithmic scale (Ridge: $\alpha \in [10^{-6},10^{6}]$ and Lasso: $[10^{-4},10]$. The combination minimizing mean cross-validated mean squared error was selected. Once optimal α was determined, models were

Downloaded from ascelibrary.org by Md Jobair Bin Alam on 03/10/26. Copyright ASCE. For personal use only; all rights reserved.

refit on the full standardized dataset. Coefficients were then back-transformed to the original variables. Model performance was assessed by the Coefficient of determination (R^2) and Root mean squared error (RMSE).

RESULTS AND DISCUSSION

The two fitted prediction equations from Ridge and Lasso regression are presented in Equations 4 and 5, respectively. Back-transformed coefficients are presented in Table 1. In every model, moisture content carries the largest magnitude, confirming it as the primary driver of resistivity changes under ET-cover conditions. Temperature is a secondary influence, and suction bears the smallest coefficient, indicating minimal marginal effect once moisture and temperature are accounted for. Here, the intercept (15.48 Ω-m) is the baseline resistivity when all predictors are zero. Each 1% increase in moisture content reduces predicted resistivity by 27.13 Ω-m, while a 1 kPa rise in matric suction and a 1°C rise in temperature reduce it by 0.92 Ω-m and 1.99 Ω-m, respectively. The relatively large magnitude of the moisture coefficient (and the fact that none of the coefficients were driven exactly to zero after standardization and tuning) shows that all three variables contribute, but moisture remains the dominant driver under L1 regularization.

Ridge Equation (α = 0.0100):

$$y = 105.3147 - 271.2358 \times x_1 - 0.0018 \times x_2 - 0.1942 \times x_3 \quad (4)$$

Lasso Equation (α = 0.0139):

$$y = 15.4823 - 27.1298 \times x_1 - 0.9223 \times x_2 - 1.9904 \times x_3 \quad (5)$$

In this L2-penalized model, the intercept (105.31 Ω-m) reflects the mean-centered baseline. A 1 % increase in moisture corresponds to a 271.24 Ω-m drop in resistivity, indicating an even stronger inverse effect once multicollinearity is mitigated, while suction's coefficient is nearly zero (–0.0018 Ω-m/kPa), confirming its negligible marginal role. Temperature retains a modest negative influence (–0.194 Ω-m/°C). In both equations, the negative signs reflect the physical fact that higher moisture, higher suction (i.e., drier conditions), and higher temperature all tend to lower bulk resistivity. The significantly larger magnitude of the moisture coefficient in both fits underscores moisture content as the primary control, whereas suction's small Ridge coefficient highlights its minimal independent effect once moisture and temperature are accounted for.

Table 1. Back-transformed model coefficients.

Model	Moisture (Ω-m / % VMC)	Suction (Ω-m / kPa)	Temperature (Ω-m / °C)
Ridge	-271.24	-0.0018	-0.1942
Lasso	-27.13	-0.9223	-1.9904

Figure 4 shows the actual and predicted resistivity. The figure illustrates how each regularized model aligns with the one-to-one line across the full range of measured resistivity. In the mid-range resistivity (≈ 30–60 Ω-m), both models cluster closely around the 1:1 line in this central band, indicating strong predictive accuracy where most of the data is located. However,

Downloaded from ascelibrary.org by Md Jobair Bin Alam on 03/10/26. Copyright ASCE. For personal use only; all rights reserved.

in the low-end resistivity (< 20 Ω-m), Ridge exhibits the smallest deviation from the reference line, while the Lasso model displays slightly greater scatter, occasionally overpredicting very low resistivities. This indicates that Ridge's L2 penalty enables it to flexibly fit the small-value tail without completely shrinking coefficients to zero. At the high-end values (> 80 Ω-m), the Ridge model stays closer to the 1:1 line, whereas Lasso tends to underpredict the highest resistivities, an artifact of L1 shrinkage that eliminates weaker predictors and thus dampens extreme fits. Overall, no significant funnel shape is evident in the residuals, suggesting homoscedastic errors and validating the linear model assumption.

Table 2 summarizes the cross-validated goodness-of-fit or quantitative metrics for all the regularized models. Ridge regression achieved the best performance (R^2 = 0.778; RMSE = 4.28 Ω-m). While the quantitative metrics of Lasso regression were R^2 = 0.692, RMSE = 9.40 Ω-m. The superiority of Ridge reflects its ability to retain all predictors while uniformly shrinking their coefficients, minimizing both bias and variance across the full resistivity range. Because Ridge retains all predictors (moisture, suction, temperature) with moderate shrinkage, it adapts best to the full resistivity spectrum. Lasso's zeroing of the moisture coefficient and the resulting loss of explanatory power at the extremes explain its slightly poorer high-end fit.

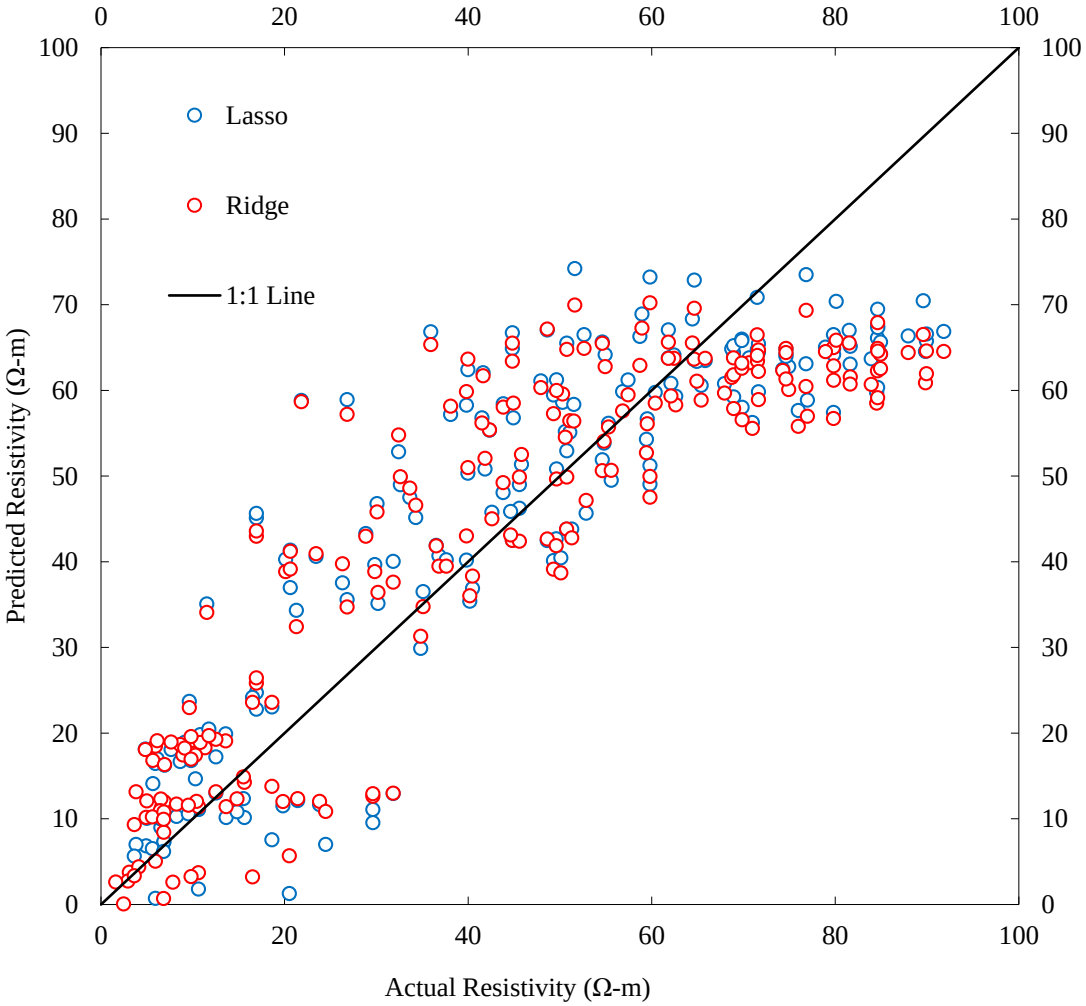

Figure 4. Actual vs Predicted Resistivity for Regularized Models

Downloaded from ascelibrary.org by Md Jobair Bin Alam on 03/10/26. Copyright ASCE. For personal use only; all rights reserved.

Downloaded from ascelibrary.org by Md Jobair Bin Alam on 03/10/26. Copyright ASCE. For personal use only; all rights reserved.

In the Ridge regression, the coefficient for suction (–0.0018 Ω·m per kPa) is over two orders of magnitude smaller than those for moisture (–271.2358 Ω·m per % vol) and temperature (–0.1942 Ω·m per °C). This disparity indicates that matric suction contributes almost no additional explanatory power to resistivity predictions once moisture content and temperature are accounted for. The L2 penalty in Ridge uniformly shrinks coefficients, yet it preserved substantial weights on moisture and temperature while driving suction nearly to zero, highlighting its negligible marginal effect. Consequently, suction's role in the final predictive model is minimal, and its inclusion would not improve model accuracy. The coefficient on suction (–0.0018) is two to five orders of magnitude smaller than the coefficients on moisture (–271.2358) and temperature (–0.1942). Even though suction varies over tens of kPa in the field-monitored dataset, its tiny per-unit coefficient means its overall contribution to predicted resistivity variance is negligible compared to moisture and temperature. Ridge shrinkage also down-weights predictors that add little unique explanatory power. Suction's low coefficient reflects both its weaker correlation with resistivity (after accounting for moisture and temperature) and the L2 penalty's uniform shrinkage. Hence, suction has the least effect on resistivity prediction in your Ridge model.

Table 2. Cross-validated R^2 and RMSE for Ridge and Lasso models

Regression Model	Coefficient of Determination (R^2)	Root Mean Square Error (RMSE)
Ridge	0.778	4.28
Lasso	0.692	9.40

LIMITATION OF THE STUDY

This analysis is limited by its reliance on only three predictors (moisture, suction, and temperature) and assumes a strictly linear relationship with resistivity; other soil properties (e.g., porosity, mineralogy) and non-linear interactions were not considered. All model fitting and validation were performed on a single dataset without an independent test set, so generalizability to other soil types or field conditions remains unverified. Regularization hyperparameters were selected via cross-validation on this same data, which may still incur some bias, especially in the tails of the resistivity distribution. Additionally, measurement error in the input sensors and the standardization step may have influenced coefficient estimates, particularly for variables on smaller scales. Finally, spatial and temporal variability, such as seasonal moisture fluctuations or spatial heterogeneity, were not explicitly modeled, potentially limiting the applicability of these equations under dynamic environmental conditions.

CONCLUSION

In conclusion, Ridge regression, using an L2 penalty of $\alpha = 0.01$, provided the strongest predictive performance for soil resistivity ($R^2 = 0.778$; RMSE = 4.28 Ω-m). By uniformly shrinking all coefficients, it retained substantial sensitivity to moisture (–271.24 Ω-m per %vol) and temperature (–0.194 Ω-m per °C) while assigning a near-zero coefficient to suction (–0.0018 Ω-m per kPa), underscoring suction's negligible independent contribution once the other variables are accounted for. By contrast, Lasso ($\alpha \approx 0.0139$) yielded a marginally lower $R^2 = 0.692$ and higher RMSE = 9.40 Ω-m, reflecting its stronger sparsity bias that, although

simplifying the model, compromises tail-end accuracy. These results indicate that for robust resistivity estimation across diverse field conditions, Ridge regression is recommended. In contrast, Lasso remains suitable only when model parsimony is critical and a slight loss of extreme-value precision is acceptable.

FUTURE WORK

While Ridge regression demonstrated strong predictive performance in estimating soil resistivity from moisture, suction, and temperature data, incorporating pore-structure-informed features can substantially enhance this modeling framework. Future work will integrate empirical data from the 3D-printed soil pore volume to validate and refine model inputs, particularly bulk density and porosity proxies derived from compaction and root penetration studies. Using segmented CT images and printed soil analogs, hydraulic conductivity and resistivity tests will be conducted to establish direct pore-volume–resistivity correlations, offering an additional layer of interpretability for machine learning algorithms.

This direction opens a pathway toward multiscale soil characterization, where machine learning predictions based on bulk field data are grounded in physical models of pore connectivity and plant-root interaction. Moreover, the fabrication techniques demonstrated in related studies on composites and thermally modeled extrusion printing offer scalable and bio-inspired strategies to simulate natural soil behavior (Akib et al., 2024; Rahman et al., 2023; Ufodike & Nzebuka, 2022). Ultimately, coupling machine learning with additive manufacturing and experimental root growth analytics holds transformative potential for applications of ERI in sustainable agriculture, green infrastructure, and smart geotechnical design.

ACKNOWLEDGEMENT

We gratefully acknowledge partial support from the Panther RISE (PRISE) Grant Program at Prairie View A&M University and Texas A&M University and from the National Science Foundation (NSF) under Grant No. 2320057. Any opinions, findings, and conclusions or recommendations expressed in this material are those of the authors and do not necessarily reflect the views of the NSF.

REFERENCES

Altelbany, S. I. (2021). “Evaluation of Ridge, Elastic Net and Lasso Regression Methods in Precedence of Multicollinearity Problem: A Simulation Study.” *J. Appl. Econ. Bus. Stud.*, 5(1), 131-142.

Akib, Y. M., Bedsole, C. O., Rahman, A. M., Hamilton, J., Khan, F., Pei, Z., Shaw, B. D., and Ufodike, C. O. (2024). “A Preliminary Experimental Study on Biodegradation of 3D-Printed Samples from Biomass–Fungi Composite Materials.” *J. Compos. Sci.*, 8(10), 412.

Alam, M. J. B., Hossain, M. S., Sarkar, L., and Rahman, N. (2019). “Evaluation of Field Scale Unsaturated Soil Behavior of Landfill Cover through Geophysical Testing and Instrumentation.” *Geotech. Spec. Publ.*, 1-11.

Archie, G. E. (1942). The electrical resistivity log as an aid in determining some reservoir characteristics. *Transactions of the AIME*, 146(01), 146(1), 54-62.

Downloaded from ascelibrary.org by Md Jobair Bin Alam on 03/10/26. Copyright ASCE. For personal use only; all rights reserved.

Bernardi, A. C. D. C., Pitrat, T., Rabello, L. M., Pezzopane, J. R. M., Bosi, C., Mazzuco, G. G., and Bettio, G. M. (2019). "Differences in soil electrical resistivity tomography due to soil water contents in an integrated agricultural system." *Pesqui. Agropecu. Bras.*, 54, e00774.

Chambers, J. E., Gunn, D. A., Wilkinson, P. B., Meldrum, P. I., Haslam, E., Holyoake, S., Kirkham, M., Kuras, O., Merritt, A., and Wragg, J. (2014). "4D electrical resistivity tomography monitoring of soil moisture dynamics in an operational railway embankment." *Near Surf. Geophys.*, 12(1), 61-72.

Coelho, V. L., Piantini, A., Altafim, R. A. C., Almaguer, H. A. D., Coelho, R. A., De Lima, M. R., Boaventura, W. D. C., Paulino, J. O. S., and Nosaki, P. L. (2013). "The influence of seasonal soil moisture on the design of grounding systems." *Proc., 2013 Int. Symp. on Lightning Protection*, 201-208.

Al Dabal, M. A. A. (2021). *A Comparative Study of Ridge, LASSO and Elastic net Estimators*. Carleton University,

Efeizomor, R. O. (2023). "A Comparative Study of Methods of Remedying Multicolinearity." *Am. J. Theor. Appl. Stat.*, 12(4), 87-91.

Herawati, N., Nisa, K., Setiawan, E., Nusyirwan, N., and Tiryono, T. (2018). "Regularized Multiple Regression Methods to Deal with Severe Multicollinearity." *Statistics*, 8(4), 167-172.

Jusoh, H., and Osman, S. B. S. (2017). The correlation between resistivity and soil properties as an alternative to soil investigation. *Indian J. Sci. Technol.*, 10(6), 1-5.

Liangfu, L., and Binquan, Q. (2012). "Research on influence of soil water content on soil resistivity." *Proc., 2012 31st Int. Conf. on Lightning Protection*, 1-7.

Nnamdi, O. S., and Chandima, G. (2023). "New Method for Modelling Seasonal Variation in Resistance and Performance of Earthing Systems." *Energies*, 16(19), 7002.

Piegari, E., and Di Maio, R. (2013). "Estimating soil suction from electrical resistivity." *Nat. Hazards Earth Syst. Sci.*, 2369-2379.

Rahmawati, F., Suratman, R. Y., and Magister, A. (2022). "Performance of Ridge Regression and Lasso Regression on Data with Multicollinearity." *Leibniz: Jurnal Mat.*, 2(2), 1-10.

Rahman, A. M., Rahman, T. T., Pei, Z., Ufodike, C. O., Lee, J., and Elwany, A. (2023). "Additive Manufacturing Using Agriculturally Derived Biowastes: A Systematic Literature Review." *Bioengineering*, 10(7), 845.

Rein, A., Hoffmann, R., and Dietrich, P. (2004). Influence of natural time-dependent variations of electrical conductivity on DC resistivity measurements. *Journal of Hydrology*, 285(1-4), 215-232.

Reddy, A. S., and Chandrasekaran, K. (2022). "Measurement of Resistivity of Soil with Moisture Level and a Frequency Function." *Proc., 2022 Int. Conf. on Intell. Controller and Comput. for Smart Power*, 1-5.

Schreiber-Gregory, D. N. (2018). "Ridge Regression and multicollinearity: An in-depth review." *Model Assist. Stat. Appl.*, 13(4), 359-365.

Sari, N., Zawawi, M. A. M., Prastowo, P., and Suharnoto, Y. (2014). "Effects of Soil Moisture Content on Groundwater Electrical Resistivity Values in Irrigation Paddy Scheme, Tanjong Karang, Malaysia." *Int. J. on Adv. Sci. Eng. and Info. Technol.*, 4(5), 340-344.

Ufodike, C. O., and Nzebuka, G. C. (2022). "Investigation of thermal evolution and fluid flow in the hot-end of a material extrusion 3D Printer using melting model." *Addit. Manuf.*, 49, 102502.

Downloaded from ascelibrary.org by Md Jobair Bin Alam on 03/10/26. Copyright ASCE. For personal use only; all rights reserved.

van Genuchten, M. T. (1980). “A Closed-form Equation for Predicting the Hydraulic Conductivity of Unsaturated Soils.” *Soil Sci. Soc. Am. J.*, 44(5), 892-898.
Zha, F., Liu, S., Du, Y., and Cui, K. (2010). “Prediction of matric suction of unsaturated soil based on electrical resistivity.” *Rock Soil Mech.*, 31(3), 1003-1008.

Downloaded from ascelibrary.org by Md Jobair Bin Alam on 03/10/26. Copyright ASCE. For personal use only; all rights reserved.